analytical chemistry

Article

Cite This: *Anal. Chem.* 2019, 91, 11821−11826

pubs.acs.org/ac

Sensitive Hyaluronidase Biosensor Based on Target-Responsive Hydrogel Using Electronic Balance as Readout

Zhixin Li,[†,⊥] Caixi Tang,[‡,⊥] Da Huang,[§] Wenjuan Qin,[*,∥] Fang Luo,[§] Jian Wang,[†] Longhua Guo,[†] Bin Qiu,[†] and Zhenyu Lin[*,†]

[†]Ministry of Education Key Laboratory for Analytical Science of Food Safety and Biology, Fujian Provincial Key Laboratory of Analysis and Detection for Food Safety, College of Chemistry, Fuzhou University, Fuzhou, Fujian 350116, China

[‡]Department of Hepatobiliary & Pancreatic Surgery, Affiliated Zhuzhou Hospital, Xiangya Medial College, CSU, Zhuzhou, Hunan 412007, China

[§]College of Biological Science and Engineering, Fuzhou University, Fuzhou, Fujian 350116, China

[∥]Department of Radiation Oncology, Zhongshan Hospital Affiliated Xiamen University, Xiamen 361001, China

Supporting Information

ABSTRACT: The development of simple but sensitive methods for hyaluronidase (HAase) detection has been paid a great deal of attention because HAase is a potential cancer marker. In this work, a novel system coupled with a controlled release system has been designed for HAase determination without complex analytical instruments and skilled technicians. Pt@SiO_2 nanoparticles (NPs), which can catalyze the breakdown of H_2O_2 into O_2 and H_2O, was embedded in the hydrogel constructed by polyethylenimine (PEI) and hyaluronic acid (HA). In the presence of HAase, the hydrogel was broken down as HAase can catalyze the degradation of HA and hence the Pt@SiO_2 NPs in the hydrogel was released. The released Pt@SiO_2 NPs mixed with H_2O_2 solution in a drainage device, and then O_2 was generated due to the decomposition of H_2O_2, resulting in an enhancement of pressure in the drainage device because of the low solubility of O_2. A certain amount of H_2O overflowed from the drainage device because the difference of the pressure between the inner and outer of the drainage device. The overflowed H_2O was collected by a tube, and its amount was easily measured by an electronic balance. The weight of the H_2O has a linear relationship with the HAase concentration in the range of 1−60 U/mL (120 min enzymatic hydrolysis time) and 0.2−10 U/mL (240 min enzymatic hydrolysis time). The developed system has been applied to detect the activity of HAase in urine samples with satisfied results.

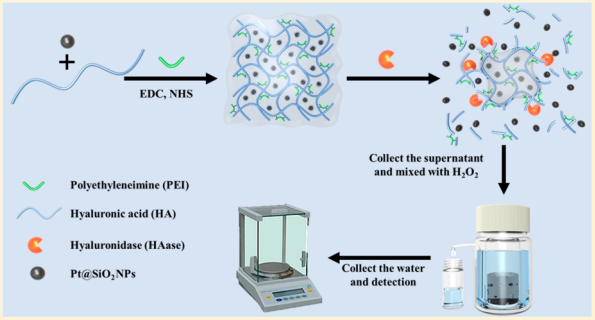

Many simple devices which can be used to measure physical parameters, such as length, temperature, pH value, pressure, and so on, have been used as readout device and coupled with different recognition strategies to develop biosensors for diverse targets.[1−8] The electronic balance, one of the most common pieces of equipment in nearly all laboratories, is frequently applied to weigh materials with high accuracy, but has rarely been adopted as readout device in the developing of biosensors. Our group has reported a novel and effective biosensor for thrombin detection based on the weight signal measured by an electronic balance.[9] But much efforts are needed to expand the application of this simple device.

Almost all trace biomarkers cannot be detected by electronic balance directly, hence signal conversion and amplification is needed. Controlled release system, which can only respond with the target or target environment and then releases plenty of signal probes, has advantages of high sensitivity, stability, and specificity. For the past few years, controlled release strategy has been coupled with various detection methods, such as colorimetry,[10,11] chemiluminescence method,[12] fluorescence method,[13,14] and so on, to detect diverse targets. Furthermore, controlled release strategy has also been applied in conjunction with a barometer,[15] a hand-held pH meter,[16] and a glucometer[17] to develop many point-of-care test systems. However, nearly no attention has been paid to the development of a controlled release biosensor using an electronic balance as signal readout.

Hyaluronic acid (HA), a type of linear glycosaminoglycan with high molecular weight, distributes widely in the extracellular matrix.[18] As a specific enzyme of HA, hyaluronidase (HAase) can catalyze the degradation of HA with high efficiency.[19] The overexpression of HAase has been found to relate with many malignancies, such as brain,[20] bladder,[21,22] prostate,[23] and colorectal cancer[24] at the early stages. Several methods have been designed for HAase detection, such as viscosimetry,[25] turbidimetry,[26] zymography,[27] etc. Recently,

Received: May 29, 2019
Accepted: August 22, 2019
Published: August 22, 2019

DOI: 10.1021/acs.analchem.9b02487
Anal. Chem. 2019, 91, 11821−11826

colorimetry,[22,28] electrochemiluminescence (ECL),[29] and fluorescence methods[30−37] have also been reported for HAase detection. Nearly all methods need relative complex analytical instruments and skilled technicians. Colorimetry is a convenient method that can detect HAase by the naked eye, but the sensitivity of which is not high enough. Therefore, more attention should be paid on the development of a simple system for HAase detection by an easily operated and easily accessed instrument with high sensitivity and selectivity.

In this work, a novel system has been designed for HAase detection using a commonly available electronic balance as readout. The proposed system relies on a target-responsive controlled release hydrogel for HAase recognition and the release of Pt@SiO_2 nanoparticles (NPs), metal catalyst (Pt@SiO_2 NPs) can catalyze the decomposition of H_2O_2 into O_2 and H_2O and, hence, produces pressure difference between the inner and outer of the drainage device because of the low solubility of the produced O_2. In this case, the discharge of a certain amount of H_2O from the system is caused and can be weighted easily and accurately by an electronic balance. The proposed system was then applied to detect activity of HAase in urine samples.

EXPERIMENTAL SECTION

Materials. Hydrogen peroxide (H_2O_2, 30 wt %), chloroplatinic acid hexahydrate ($H_2PtCl_6·6H_2O$), 1-(3-(dimethylamino)propyl)-3-ethylcarbodiimide hydrochloride (EDC), ascorbic acid, polyethylenimine (PEI), *N*-hydroxysuccinimide (NHS), glutathione (GSH), and trypsin (Try) were purchased from Aladdin Bio-Chem Technology Co., Ltd. (Shanghai China). HAase (from bovine testes, 400 U/mg), HA (from rooster comb), and alkaline phosphatase (ALP) were obtained from Sigma-Aldrich. *N*-Hexyl alcohol, $MgCl_2$, $CaCl_2$, ethyl orthosilicate (TEOS), and triton X-100 were obtained from Sinopharm Chemical Reagent Co., Ltd. (China). 20× phosphate buffered saline (PBS), and lysozyme (Lyz) was obtained from Shanghai Sangon Biotechnology Co., Ltd. (Shanghai, China). Cyclohexane, acetone, ammonium hydroxide, and ethanol were purchased from Fuchen Chemical Reagent Co., Ltd. (Tianjin, China). NaCl, KCl, urea, and glucose (Glu) was purchased from Xilong Scientific Co., Ltd. (Guangdong, China). Uric acid (UA) was obtained from Tokyo Chemical Industry Co., Ltd. (Tokyo, Japan). L-Threonine (Thr), cytochrome c (Cyt c), human serum albumin (HAS), was obtained from Macklin Biochemical Co., Ltd. (Shanghai, China). All other chemicals were at least analytical grade reagents and used directly without further purification. All solutions were prepared with deionized H_2O (Milli-Q, Millipore, resistance 18.2 MΩ·cm).

Apparatus. TMS-200 Thermo shaker incubator was purchased from Allsheng Instruments Co., Ltd. (Hangzhou, China). MS 3 digital small shaker was obtained from IKA (Janke& Kunkel KG.IKA-werk, Staufen, Germany). An electronic balance (Sartorius, BT25s, China) with an accuracy of 0.01 mg was used to record the weight. Glass vials and plastic vials with screw caps were purchased from Hemei instrument technology (Jiangsu, China). An enzyme-linked immunosorbent assay (ELISA) kit for HAase was obtained from Shanghai Enzyme-linked Biotechnology Co., Ltd. (Shanghai, China). Transmission electron microscopy (TEM, Tecnai G2 F20 S-TWIN, FEI, Hillsboro, OR) and field emission scanning electron microscope (FESEM, Nova NanoSEM 230, FEI) was used for characterization.

Synthesis of Pt@SiO_2 NPs. Pt@SiO_2 NPs were prepared according to the early reported procedures.[38] Pt NPs were synthesized just by mixing H_2PtCl_6 (2 mL, 18.9 mM) and ascorbic acid (1.5 mL, 0.4 mM) together in a beaker. After being heated in a water bath at 80 °C for 20 min, the brown suspension containing monodisperse and well-defined Pt NPs was obtained. The suspension was concentrated to 150 μL through centrifugation and mixed with the solution including triton x-100 (7.08 mL), *n*-hexyl alcohol (7.20 mL), cyclohexane (30.0 mL), and H_2O (1.36 mL). After that, TEOS (400 μL) and $NH_3·H_2O$ (240 μL) were mixed with the above solution mixture and shaken evenly for 24 h. Then the resulting suspension was centrifuged, and the precipitates were washed with distilled water and ethanol and then being dried, weighted, and dispersed in H_2O for later use (30 mg/mL).

Fabrication of HA-PEI Hydrogel Embedded with Pt@SiO_2 NPs. HA sodium salt solution (4 μL, 1%) was mixed with Pt@SiO_2 NPs (2 μL, 30 mg/mL), EDC (2 μL, 48.8 mg/mL), NHS (2 μL, 11.5 mg/mL), and 4 μL H_2O in the centrifuge tube (200 μL), and then the mixed solution was shaken 15 min to activate carboxylic group of HA. Next, PEI (2 μL, 0.4%) was added to the above solution and reacted with activated HA for 120 min. After that, the hydrogel was formed in the centrifuge tube through the chemical bond between HA and PEI for the later use.

Procedures of HAase Detection. Different concentration of HAase solution (60 μL) was added on the top of the hydrogel in the centrifuge tube separately, and then the centrifuge tube was turned upside-down and incubated at 37 °C to enable HAase digest the HA in the hydrogel. After 120 min enzymatic hydrolysis, 50 μL of supernatant was collected and mixed with H_2O_2 solution (1 mL) in a small glass vial (5 mL), and then the small glass vial was placed in a big plastic vial (20 mL) sealed with a cap containing a silicon, and the top of glass vial and plastic vial were interlinked. The part between the small glass vial and the big plastic vial was filled with H_2O (∼10.0 mL), and a pipe connecting with the atmosphere was inserted into the bottom of the plastic vial. O_2 was generated due to the decomposition of H_2O_2, resulting in an enhancement of pressure inside the plastic vial. A certain amount of H_2O pushed from the pipe with the increase of pressure was collected and measured by an electronic balance. Each sample was detected three times, and the average value was calculated for quantitative analysis. Unless otherwise mentioned, the entire project was carried out at room temperature.

RESULTS AND DISCUSSION

Principle of the Proposed Biosensor for Hyaluronidase. Scheme 1 shows the principle of the biosensor. Carboxyl group activated by EDC and NHS can combine with the amino group to form amide bond, hence carboxyl-rich HA and amine-rich PEI can be used to construct hydrogels through the formation of plenty of amide bonds. Pt@SiO_2 NPs, which can catalyze the decomposition of H_2O_2 into O_2 and H_2O, was embedded in the hydrogel first. In the presence of HAase, HA in the hydrogel can be digested by HAase, leading to the disruption of the hydrogel, and then Pt@SiO_2 NPs can be released from the hydrogel into supernatant. The drainage device consists of two bottles. The inner bottle contains H_2O_2 solution and the outer bottle contains water. An appropriate amount of supernatant is collected and droped in the H_2O_2 solution and the outer bottle is capped. The O_2 generated due to the decomposition of H_2O_2 is nearly insoluble in water,

DOI: 10.1021/acs.analchem.9b02487
Anal. Chem. 2019, 91, 11821−11826

Scheme 1. Schematic Illustration of the Proposed Hydrogel Biosensor for HAase Detection

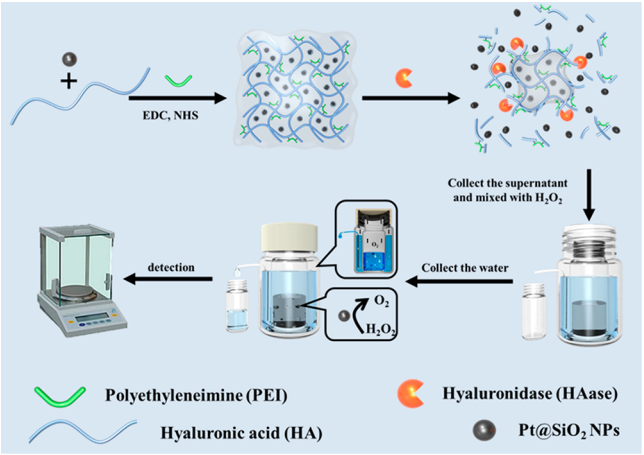

resulting in an enhancement of pressure in the drainage device. Therefore, certain amount of H_2O overflowed because of the difference of the pressure between the drainage device and outer area, which can be collected and measured by electronic balance easily. The concentration of HAase affects the amount of $Pt@SiO_2$ NPs released from the hydrogel, and the amount of $Pt@SiO_2$ NPs is closely related to the amount of H_2O collected from the drainage device. Therefore, a close relationship between the weight of H_2O and the concentration of HAase can be established for HAase detection. In this case, a simple method can be developed for HAase detection.

TEM of $Pt@SiO_2$ NPs and $Pt@SiO_2$ NPs embedded into the HA-PEI hydrogel were shown in Supporting Information (SI) Figure S1. The $Pt@SiO_2$ NPs had a uniform size with an average size around 120 nm (SI Figure S1A). When $Pt@SiO_2$ NPs was added in the hydrogel, it can be observed clearly that the $Pt@SiO_2$ NPs was wrapped by a thin membrane, indicating that $Pt@SiO_2$ NPs was embedded into the hydrogel. Besides that, SEM of HA-PEI hydrogel and HA-PEI hydrogel embedded with $Pt@SiO_2$ NPs was provided in SI Figure S2 to further prove the $Pt@SiO_2$ NPs were embedded in the hydrogel. The surface of HA-PEI hydrogel without $Pt@SiO_2$ NPs was smooth (SI Figure S2A). When $Pt@SiO_2$ NPs was added in the hydrogel, plenty of spherical protuberances can be observed on the surface of hydrogel (SI Figure S2B), demonstrating that the $Pt@SiO_2$ NPs were embedded in the hydrogel successfully.

Simple control assay was carried out to verify the feasibility of our presumption. As shown in Figure 1A, in the absence of HAase, the hydrogel was not broken down. In contrast, the hydrogel was hydrolyzed in the presence of HAase, and the volume of hydrogel was decreased significantly. As shown in Figure 1B, in the absence of HAase, the mixed solution containing supernate and H_2O_2 solution did not produce any bubbles. In the presence of HAase, a large amount of bubbles were produced in the mixed solution containing supernate and H_2O_2, resulting in an enhancement of pressure in the drainage device. The weight of the collected water is shown in Figure 1C, no water was collected in the absence of HAase, however in the presence of HAase, plenty of water was pushed out from the drainage device and collected, and this outcome can be applied to imply the existence of HAase. All these phenomena show that the hydrogel cannot be broken down in the absence of HAase, and the $Pt@SiO_2$ NPs embedded in hydrogel has high stability, confirming the principle of the proposed presumption.

Optimization of the Reaction Conditions. To achieve the best sensing performance, several parameters were optimized. The mass fraction ratio of PEI to HA is crucial to the performance of the hydrogel. Low proportion of PEI can reduce the stability of the hydrogel and therefore leads to the release of $Pt@SiO_2$ NPs from the hydrogel. The $Pt@SiO_2$ NPs escaped from the hydrogel can result a high background signal. In contrast, high proportion of PEI can enable few $Pt@SiO_2$ NPs to be released from the hydrogel in a certain enzymolysis time and then affects the sensitivity of the hydrogel biosensor. Therefore, different mass fraction of PEI (2 μL) was added for the hydrogel synthesis and then applied to detect HAase. As shown in Figure 2A, in the presence of HAase (40 U/mL), the weight of H_2O increased with the decrease of mass fraction ratio of PEI to HA. The result indicated that lower mass fraction of PEI can form fewer amide bonds in the hydrogel with HA which can enable the hydrogel to be easily broken down in a short time. When the mass fraction ratio of PEI to HA was decreased from 0.2 to 0.15, $Pt@SiO_2$ NPs escaped from the hydrogel in the absence of HAase, and the H_2O was collected as background signal. Such outcome showed that the mass fraction of PEI is too low to maintain the stability of hydrogel through the amide bond formation, and as a result, the background signal was generated by the $Pt@SiO_2$ NPs escaped from the hydrogel. Therefore, 0.2 is the best mass fraction ratio of PEI to HA, which can generate the largest signal without background.

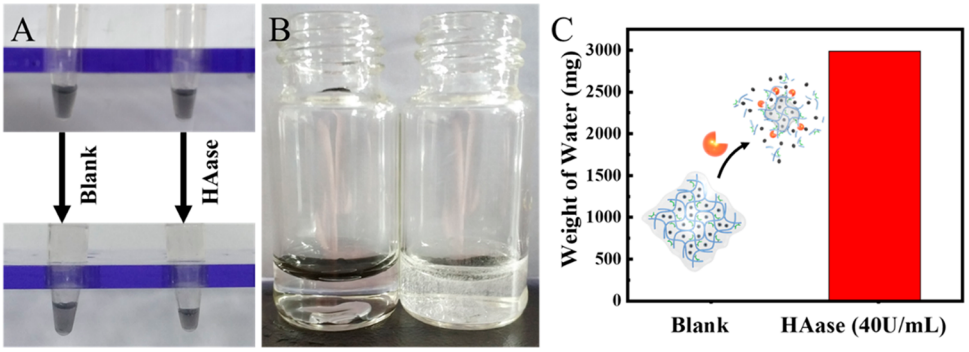

Figure 1. Change of the hydrogel volume (A), the bubble produced from the H_2O_2 solution mixed with supernate (B), and the weight of the water collected from the glass vials (C) with and without HAase.

DOI: 10.1021/acs.analchem.9b02487
Anal. Chem. 2019, 91, 11821−11826

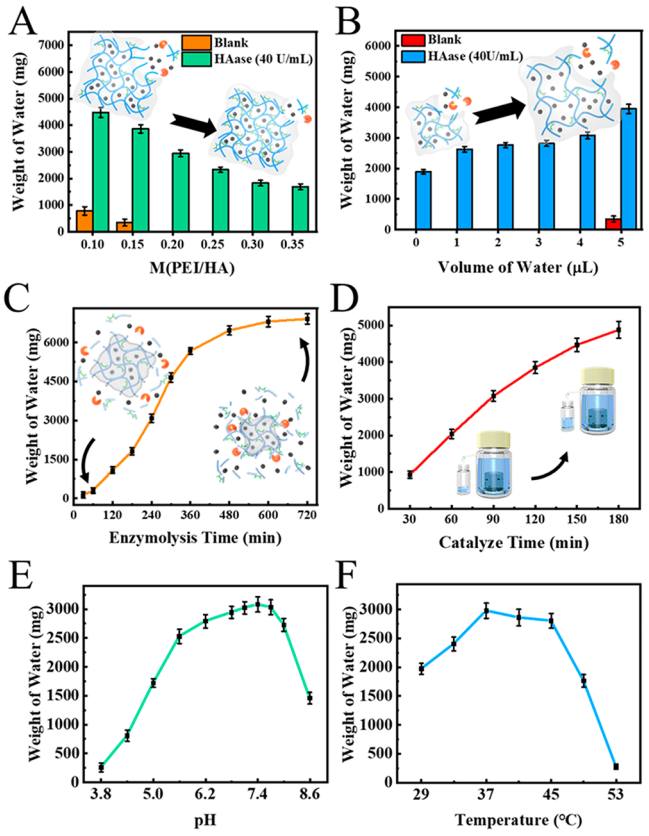

Figure 2. (A) The relationship between the volumes of water collected from drainage device and mass fraction ratio of PEI to HA. (B) The relationship between the volumes of water collected from drainage device and volume of water added for hydrogel synthesis. (C) The relationship between the weight of water collected from drainage device and enzymolysis time. (D) The relationship between the weight of water collected from drainage device and catalyzation time. (E) The relationship between the weight of water collected from drainage device and the pH in enzymolysis process. (F) The relationship between the weight of water collected from drainage device and the temperature in enzymolysis process. Error bars represent the standard deviations for three replicates.

The three-dimensional network structures of hydrogel can also significantly affect the hydrogel performance. Low density of the three-dimensional network structures of the hydrogel can cause escape of Pt@SiO_2 NPs from hydrogel in the absence of HAase and, hence, produces the background signal, ultimately reducing the stability of the hydrogel biosensor. High density of the three-dimensional network structures of the hydrogel may reduce the hydrolysis efficiency of HAase and makes the release of the Pt@SiO_2 NPs more difficult, ultimately reducing the sensitivity of the hydrogel biosensor. Therefore, to achieve the best sensing performance, different volumes of H_2O was added to participate in hydrogel synthesis to change the ultimate hydrogel volume and then affect the density of the three-dimensional network structures of the hydrogel. The above-mentioned hydrogel was used for 40 U/mL HAase detection. As shown in Figure 2B, and the weight of water collected increased with the increase of the H_2O content of the hydrogel, indicating that lower density of the three-dimensional network structures of the hydrogel could make Pt@SiO_2 NPs release easier. When the volume of H_2O that was added to participate in hydrogel synthesis increased to 7 μL, Pt@SiO_2 NPs was released from the hydrogel in the absence of HAase because of low density of the three-dimensional network structures of the hydrogel, resulting in a relatively high background signal. Therefore, 6 μL of H_2O was added to participate in hydrogel synthesis for reducing the three-dimensional network structure density of the hydrogel, which can generate the largest signal without background.

The enzymolysis time between HAase and hydrogel also greatly affects the performance of the proposed biosensor. Longer enzymolysis time can make more Pt@SiO_2 NPs release from hydrogel, and then more water can be collected, but the detection progress requires more time. Therefore, to find an appropriate condition, the proposed biosensor was applied to detect HAase (10 U/mL) at different enzymolysis time. As shown in Figure 2C, the weight of water increased with the increase of enzymolysis time, suggesting that the longer time the hydrogel is cleaved by HAase, the more Pt@SiO_2 NPs can be released from hydrogel. Therefore, a short enzymolysis time can be applied for rapid detection of high concentration of HAase in a sample, and a long enzymolysis time can be used to detect low concentration of HAase to improve the sensitivity of the biosensor. In this work, 120 min was chosen as the enzymolysis time of high concentration HAase detection (1−60 U/mL), 240 min was chosen as the enzymolysis time of low concentration HAase detection (0.2−10 U/mL).

Similarly, catalyzation time between H_2O_2 and Pt@SiO_2 NPs that can influence the performance of the proposed biosensor should be optimized as well. A long enzymolysis time that can collect a large amount of water can be used to improve the sensitivity of the biosensor, but it can reduce the efficiency of HAase detection. To find appropriate catalyzation time, 40 U/mL of HAase (enzymolysis time was 120 min) was detected by the biosensor with different catalyzation times. As shown in Figure 2D, the weight of water increased with the increase of catalyzation time. So 90 min was selected to reach the requirement of the detection.

Temperature and pH are key factors which have a huge influence on the performance of the proposed biosensor. Therefore, different pH and temperature in enzymolysis process (40 U/mL HAase) was studied for optimal conditions. As shown in Figure 2E, the weight of water collected from the drainage device was increased as a whole with the increasing pH value from 3.8 to 6.8, and reached a plateau from 6.8 to 7.7, and then decreased with the pH value over 7.7, because of that, HAase has a low activity for HA-PEI hydrogel decomposition at acidic and alkaline conditions and has a higher activity at neutral conditions. The results indicated that pH 7.4 was the optimized condition for the enzymolysis process. The effect of temperature in enzymolysis process is shown in Figure 2F, the weight of water collected from the drainage device was increased with the increasing temperature from 29 to 37 °C and reached plateau from 37 to 45 °C, and then decreased with temperature over 45 °C. Because lower or higher temperature reduced the activity of HAase. The results indicated that 37 °C was the optimized condition for enzymolysis process. In conclusion, the biosensor has the best performance when the enzymolysis process was carried at 37 °C (pH 7.4).

Performance of the Proposed System. The weight of the water collected was measured in the presence of varying concentration of HAase under the optimized conditions (enzymolysis time was 120 min). As shown in Figure 3A, the weight of the water increased gradually with the increase of HAase concentration. There was a linear relationship between

DOI: 10.1021/acs.analchem.9b02487
Anal. Chem. 2019, 91, 11821−11826

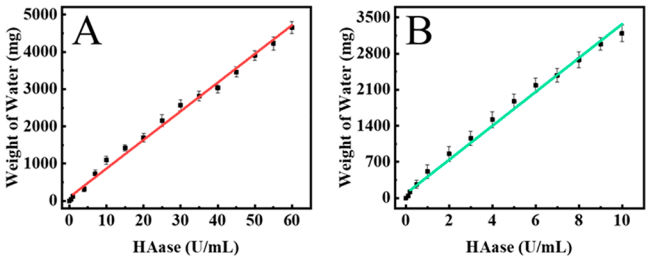

Figure 3. (A) The linear relationship between the weight of water and the HAase concentrations under 120 min enzymolysis time. (B) The linear relationship between the weight of water and low HAase concentrations under 240 min enzymolysis time. Error bars represent the standard deviations for three replicates.

the weight of the water and HAase concentration in the range of 1−60 U/mL. The linear equation is as follows

$$W_{wA}/\text{mg} = 77.00 \quad C_{HAase} + 97.21 \quad R = 0.9969 \qquad (1)$$

To detect low concentration of HAase, the time of enzymatic hydrolysis between HA and HAase was extended to 240 min to obtain more Pt@SiO_2 NPs released from hydrogel. And there was a linear relationship between the weight of the water and low HAase concentration in the range of 0.2−10 U/mL (Figure 3B). The linear equation is as follows

$$W_{wB}/\text{mg} = 329.06 \quad C_{HAase} + 82.70 \quad R = 0.9976 \qquad (2)$$

where W_{wA} and W_{wB} are the weight of water collected from drainage device in different enzymatic hydrolysis times (120 and 240 min, respectively). C_{HAase} is the HAase concentration, and R is the correlation coefficient. The limit of detection (LOD) is 1 U/mL (enzymolysis time was 120 min) and 0.2 U/mL (enzymolysis time was 240 min), respectively (the LOD was calculated according to the signal which is equivalent to 3 times of the noise). Compared with most of other methods for HAase detection (shown in SI Table S1), the current method has wide linear range and sufficient sensitivity. The LOD was comparable to some fluorescence and ECL methods. Although the detection time in this work is a little longer, compared with other reported methods, the current method does not depend on costly instruments and professional technicians, which has advantages in applications in developing regions.

To test the selectivity of the hydrogel biosensor, various potential interfering substances in urine and serum samples were selected as models. Such as inorganic salts (NaCl, KCl, $MgCl_2$, and $CaCl_2$), small molecules (Glu, GSH, Thr, urea, and UA), and bio macromolecules (Cyt c, HAS, Lyz, Try, ALP). As shown in Figure 4, no water was collected in the presence of interferences only (same as that of the blank), whereas the addition of HAase resulted in a plenty of water, confirming that the hydrogel biosensor has strong anti-interference capability.

To test the stability of the hydrogel biosensor, the hydrogel biosensor stored at 4 °C for 4 weeks and then applied to detect HAase (10 U/mL). Nearly no change was observed as compared with the freshly prepared biosensor, which indicates the proposed method has good stability.

Application of the Proposed Biosensor. To evaluate the performance of the proposed hydrogel biosensor, HAase in human urine (healthy people and patients, donated by the volunteers) was measured by the proposed system. Standard addition recovery rate was obtained to verify the accuracy of the proposed system. As shown in Table 1, the concentration of HAase in the urine sample of patients (32.95 U/mL, 26.43 U/mL, and 36.61 U/mL) was much higher than that in the heathy people (1.73 U/mL, 3.14 U/mL, and 1.29 U/mL), demonstrating that HAase as a clinical biomarker is overexpressed in tumors. Moreover, the recovery rates of HAase in urine samples were in the range of 96.74−106.80% and the RSD (n = 3) was lower than 7.9%. Besides that, a commercial ELISA kit was used to detect HAase in the same urine samples for a comparison. The results showed no significant difference between the two methods. All these results indicated that the proposed method is practical for quantitative determination of HAase in biological samples.

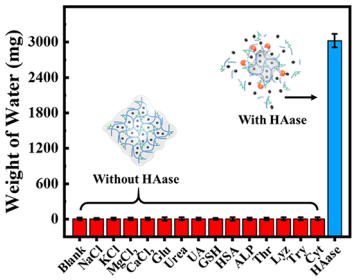

Figure 4. Weight of the water collected under the different potential interfering substances and HAase. Blank, NaCl (10 mM), KCl (10 mM), $MgCl_2$ (10 mM), $CaCl_2$ (10 mM), Glu (10 mM), GSH (10 mM), Thr (10 nM), Urea (10 mM), UA (10 mM), HSA (100 nM), Cyt c (100 nM), Lyz (100 nM), Try (100 nM), ALP (100 nM), and HAase (40 U/mL). Error bars represent the standard deviations for three replicates.

Table 1. Determination of the HAase Level in Human Urine Samples Collected from Healthy People and Cancer Patients by the Proposed Method and ELISA Method. (n = 3)

urine samples		spiked (U/mL)	detected by current method (U/mL)	recovery rate (%)	RSD (%)	detected by ELISA Method (U/mL)
healthy people	1	0	1.73		5.6	1.90
		5.0	6.94	104.20	6.9	6.82
		10.0	11.66	99.32	4.5	11.98
		15.0	17.75	106.80	5.2	16.89
	2	0	3.14		5.7	2.88
		5.0	8.27	102.56	3.3	7.88
		10.0	13.05	99.09	3.7	12.75
		15.0	18.78	104.27	6.0	17.98
	3	0	1.29		6.3	1.15
		5.0	6.32	100.61	5.1	6.18
		10.0	11.59	103.03	4.8	11.14
		15.0	17.27	106.52	7.9	16.21
cancer patients	1	0	32.95		4.3	31.51
		5.0	37.79	96.74	4.2	36.33
		10.0	43.18	102.27	2.5	41.59
		15.0	48.61	104.38	3.4	47.02
	2	0	26.43		6.1	27.39
		5.0	31.62	103.79	5.6	32.39
		10.0	37.04	106.09	3.8	37.77
		15.0	42.13	104.70	4.4	41.98
	3	0	36.61		5.8	38.43
		5.0	41.65	100.85	3.1	43.10
		10.0	47.24	106.30	4.9	49.02
		15.0	51.94	102.21	3.7	53.63

DOI: 10.1021/acs.analchem.9b02487
Anal. Chem. 2019, 91, 11821−11826

CONCLUSION

In summary, a simple, convenient, and stable system has been developed for HAase detection coupled with a controlled release system. The synthesis of the hydrogel biosensor is rapid and simple. The weight of the signal generated and amplified by drainage device can be detected byan electronic balance with high accuracy. Moreover, the sensitivity can be enhanced by increasing enzymolysis time and catalyzation time easily. The detection process is convenient and user-friendly. To the best of our knowledge, it is the first report that the HAase in human urine samples is demonstrated to be detected by a hydrogel biosensor without background signal by using an electronic balance as readout with satisfactory results. Furthermore, the novel system skillfully combines controlled release hydrogel with a low-cost and accurate electronic balance, which provides a new method for a wider detection of some biomarkers in developing regions.

ASSOCIATED CONTENT

Supporting Information

The Supporting Information is available free of charge on the ACS Publications website at DOI: 10.1021/acs.analchem.9b02487.

Additional information as noted in the text PDF)

AUTHOR INFORMATION

Corresponding Authors

*(W.J.Q.) E-mail: proftomato@163.com.

*(Z.Y.L.) E-mail: zylin@fzu.edu.cn.

ORCID

Fang Luo: 0000-0003-1480-0677

Longhua Guo: 0000-0003-0706-0973

Zhenyu Lin: 0000-0001-7890-6812

Author Contributions

⊥Z.L. and C.T. contributed equally to this work.

Notes

The authors declare no competing financial interest.

ACKNOWLEDGMENTS

This project was financially supported by National Sciences Foundation of China (21775026,21575025, 21575027), the Program for Changjiang Scholars and Innovative Research Team in University (No. IRT15R11), and the cooperative project of production and study in University of Fujian Province (2018Y4007), the Sciences Foundation of Fujian Province (2018J01685, 2018J01682), STS Key Project of Fujian Province (2017T3007).

REFERENCES

(1) Song, Y.; An, Y.; Liu, W.; Hou, W.; Li, X.; Lin, B.; Zhu, Z.; Ge, S.; Yang, H.-h.; Yang, C. *Chem. Commun.* **2017**, *53*, 11774−11777.

(2) Li, J.; Jiang, H.; Rao, X.; Liu, Z.; Zhu, H.; Xu, Y. *Anal. Chem.* **2019**, *91*, 1494−1500.

(3) Liu, D.; Li, X.; Zhou, J.; Liu, S.; Tian, T.; Song, Y.; Zhu, Z.; Zhou, L.; Ji, T.; Yang, C. *Biosens. Bioelectron.* **2017**, *96*, 332−338.

(4) Wang, L.; Chen, C.; Huang, H.; Huang, D.; Luo, F.; Qiu, B.; Guo, L.; Lin, Z.; Yang, H. *Biosens. Bioelectron.* **2018**, *121*, 153−158.

(5) Wu, R.; Ge, H.; Liu, C.; Zhang, S.; Hao, L.; Zhang, Q.; Song, J.; Tian, G.; Lv, J. *Talanta* **2019**, *196*, 191−196.

(6) Fu, G.; Sanjay, S. T.; Dou, M.; Li, X. *Nanoscale* **2016**, *8*, 5422−5427.

(7) Zhang, J.; Xing, H.; Lu, Y. *Chem. Sci.* **2018**, *9*, 3906−3910.

(8) Wei, X.; Zhou, W.; Sanjay, S. T.; Zhang, J.; Jin, Q.; Xu, F.; Dominguez, D. C.; Li, X. *Anal. Chem.* **2018**, *90*, 9888−9896.

(9) Wang, A.; Ma, X.; Ye, Y.; Luo, F.; Guo, L.; Qiu, B.; Lin, Z.; Chen, G. *Anal. Chem.* **2018**, *90*, 1087−1091.

(10) Lin, H.; Zou, Y.; Huang, Y.; Chen, J.; Zhang, W. Y.; Zhuang, Z.; Jenkins, G.; Yang, C. J. *Chem. Commun.* **2011**, *47*, 9312−9314.

(11) Nam, J.; Jung, I.-B.; Kim, B.; Lee, S.-M.; Kim, S.-E.; Lee, K.-N.; Shin, D.-S. *Sens. Actuators, B* **2018**, *270*, 112−118.

(12) Lin, Y.; Wang, X.; Sun, Y.; Dai, Y.; Sun, W.; Zhu, X.; Liu, H.; Han, R.; Gao, D.; Luo, C. *Sens. Actuators, B* **2019**, *289*, 56−64.

(13) Wu, R.; Zhang, S.; Zhang, Q.; Liu, C.; Tian, G.; Lv, J. *Sens. Actuators, B* **2019**, *282*, 750−755.

(14) Xie, X.; Szilagyi, I.; Zhai, J.; Wang, L.; Bakker, E. *ACS Sens.* **2016**, *1*, 516−520.

(15) Liu, D.; Jia, S.; Zhang, H.; Ma, Y.; Guan, Z.; Li, J.; Zhu, Z.; Ji, T.; Yang, C. J. *ACS Appl. Mater. Interfaces* **2017**, *9*, 22252−22258.

(16) Zhao, M.; Wang, P.; Guo, Y.; Wang, L.; Luo, F.; Qiu, B.; Guo, L.; Su, X.; Lin, Z.; Chen, G. *Talanta* **2018**, *176*, 34−39.

(17) Yan, L.; Zhu, Z.; Zou, Y.; Huang, Y.; Liu, D.; Jia, S.; Xu, D.; Wu, M.; Zhou, Y.; Zhou, S.; Yang, C. J. *J. Am. Chem. Soc.* **2013**, *135*, 3748−3751.

(18) Lapcik, L.; Lapcik, L.; De Smedt, S.; Demeester, J.; Chabrecek, P. *Chem. Rev.* **1998**, *98*, 2663−2684.

(19) Kramer, M. W.; Escudero, D. O.; Lokeshwar, S. D.; Golshani, R.; Ekwenna, O. O.; Acosta, K.; Merseburger, A. S.; Soloway, M.; Lokeshwar, V. B. *Cancer* **2011**, *117*, 1197−1209.

(20) Martinez-Quintanilla, J.; He, D.; Wakimoto, H.; Alemany, R.; Shah, K. *Mol. Ther.* **2015**, *23*, 108−118.

(21) Lokeshwar, V. B.; Young, M. J.; Goudarzi, G.; Iida, N.; Yudin, A. I.; Cherr, G. N.; Selzer, M. G. *Cancer Res.* **1999**, *59*, 4464−4470.

(22) Nossier, A. I.; Eissa, S.; Ismail, M. F.; Hamdy, M. A.; Azzazy, H. M. E.-S. *Biosens. Bioelectron.* **2014**, *54*, 7−14.

(23) Benitez, A.; Yates, T. J.; Lopez, L. E.; Cerwinka, W. H.; Bakkar, A.; Lokeshwar, V. B. *Cancer Res.* **2011**, *71*, 4085−4095.

(24) Bouga, H.; Tsouros, I.; Bounias, D.; Kyriakopoulou, D.; Stavropoulos, M. S.; Papageorgakopoulou, N.; Theocharis, D. A.; Vynios, D. H. *BMC Cancer* **2010**, *10*. DOI: 10.1186/1471-2407-10-499

(25) Vercruysse, K. P.; Lauwers, A. R.; Demeester, J. M. *Biochem. J.* **1995**, *306*, 153−160.

(26) Derrante, N. *J. Biol. Chem.* **1956**, *220*, 303−306.

(27) Steiner, B.; Cruce, D. *Anal. Biochem.* **1992**, *200*, 405−410.

(28) Kim, J. W.; Kim, J. H.; Chung, S. J.; Chung, B. H. *Analyst* **2009**, *134*, 1291−1293.

(29) Li, Z.; Chen, H.; Zhuo, Z.; Huang, D.; Luo, F.; Chen, L.; Wang, J.; Gun, L.; Qiu, B.; Lin, Z. *Sens. Actuators, B* **2018**, *275*, 409−414.

(30) Gu, W.; Yan, Y.; Zhang, C.; Ding, C.; Xian, Y. *ACS Appl. Mater. Interfaces* **2016**, *8*, 11272−11279.

(31) Chib, R.; Mummert, M.; Bora, I.; Laursen, B. W.; Shah, S.; Pendry, R.; Gryczynski, I.; Borejdo, J.; Gryczynski, Z.; Fudala, R. *Anal. Bioanal. Chem.* **2016**, *408*, 3811−3821.

(32) Wang, Z.; Li, X.; Song, Y.; Li, L.; Shi, W.; Ma, H. *Anal. Chem.* **2015**, *87*, 5816−5823.

(33) Cheng, D.; Han, W.; Yang, K.; Song, Y.; Jiang, M.; Song, E. *Talanta* **2014**, *130*, 408−414.

(34) Li, X.; Zhou, Z.; Tang, Y.; Zhang, C. C.; Zheng, Y.; Gao, J.; Wang, Q. *Sens. Actuators, B* **2018**, *276*, 95−100.

(35) Liu, Q.; Yan, X.; Lai, Q.; Su, X. *Sens. Actuators, B* **2019**, *282*, 45−51.

(36) Liu, S.; Zhao, N.; Cheng, Z.; Liu, H. *Nanoscale* **2015**, *7*, 6836−6842.

(37) Yang, W.; Ni, J.; Luo, F.; Weng, W.; Wei, Q.; Lin, Z.; Chen, G. *Anal. Chem.* **2017**, *89*, 8384−8390.

(38) Almana, N.; Phivilay, S. P.; Laveille, P.; Hedhili, M. N.; Fornasiero, P.; Takanabe, K.; Basset, J.-M. *J. Catal.* **2016**, *340*, 368−375.